Taylor & Francis
Taylor & Francis Group

Journal of Biomolecular Structure and Dynamics

ISSN: (Print) (Online) Journal homepage: https://www.tandfonline.com/loi/tbsd20

Synthesis, antimicrobial activity, molecular docking and ADMET study of a caprolactam-glycine cluster

Sefa Celik, Ali Tugrul Albayrak, Sevim Akyuz, Aysen E. Ozel & Belgi Diren Sigirci

To cite this article: Sefa Celik, Ali Tugrul Albayrak, Sevim Akyuz, Aysen E. Ozel & Belgi Diren Sigirci (2021) Synthesis, antimicrobial activity, molecular docking and ADMET study of a caprolactam-glycine cluster, Journal of Biomolecular Structure and Dynamics, 39:7, 2376-2386, DOI: 10.1080/07391102.2020.1748112

To link to this article: https://doi.org/10.1080/07391102.2020.1748112

JOURNAL OF BIOMOLECULAR STRUCTURE AND DYNAMICS
2021, VOL. 39, NO. 7, 2376–2386
https://doi.org/10.1080/07391102.2020.1748112

Synthesis, antimicrobial activity, molecular docking and ADMET study of a caprolactam-glycine cluster

Sefa Celik[a], Ali Tugrul Albayrak[b], Sevim Akyuz[c], Aysen E. Ozel[a] and Belgi Diren Sigirci[d]

[a]Physics Department, Science Faculty, Istanbul University, Vezneciler, Istanbul, Turkey; [b]Chemical Engineering Department, Engineering Faculty, Istanbul University-Cerrahpasa, Istanbul, Turkey; [c]Physics Department, Science and Letters Faculty, Istanbul Kultur University, Istanbul, Turkey; [d]Department of Microbiology, Faculty of Veterinary Medicine, Istanbul University-Cerrahpasa, Istanbul, Turkey

Communicated by Ramaswamy H. Sarma

ABSTRACT

Density functional theory calculations were performed with DFT method using both b3lyp/6-311++G(d,p) and wb97xd/6-311++G(d,p) levels of theory to predict the molecular geometry, to evaluate the molecular electrostatic potential and frontier molecular orbitals of synthesized a new compound: caprolactam-glysine cluster (CL-Gly). Molecular docking study of the CL-Gly was carried out to clarify the interaction and the probable binding modes, between the title compound and DNA. The antibacterial activities of CL-Gly cluster against Gram-positive and Gram-negative bacteria was determined. In silico ADMET study was also performed for predicting pharmacokinetic and toxicity profile of the synthesized cluster which expressed good drug-like behavior and non-toxic nature. It was revealed that the compound has importance in drug discovery process.

ARTICLE HISTORY
Received 19 March 2020
Accepted 21 March 2020

KEYWORDS
Antimicrobial activity; caprolactam; DFT calculations; glycine; molecular docking

1. Introduction

Glycine (Gly) is one of the simplest amino acid in the white crystalline solid form, containing a carboxyl and an amine group and having a melting point of 290 °C (Atkinson & Hibert, 2001; Oxtoby et al., 2011). Gly also has antibacterial activity. For example, in a study (Minami et al., 2004) investigating the effect of glycine on Helicobacter pylori bacteria that cause gastritis and ulcers in the stomach (Roesler, 2016), glycine has been shown to have a stronger (synergistic) antibacterial activity on bacteria if used in combination with antibiotics. In another study (Sepahi et al., 2017), glycine alone or in combination with poly-1-arginine (PLA) has been reported to exhibit toxicity against *Escherichia coli* O157: H7 and *Staphylococcus aureus* bacteria. In a patent (Bontenbal & de Bert, 2006) on the biological activity of glycine, it is reported that glycine alone, glycine salts and glycine esters show antibacterial activity against harmful pathogens in foods and beverages. Mahmoud et al.(2015) prepared a series of ternary complexes composed of glycine, anti-inflammatory drug lornoxicam and transition metal chlorides and it turned out that all the complexes except Cr (III) complex showed toxic effects against breast carcinomas (MCF7 cell line). It has been found that glycine-rich proteins available in sea hare eggs have an inhibitory effect against U937 leukemia cell line (Lee et al., 2016). Besides, studies of biological activity concerning glycine derivatives have been carried out. In a study (Cosquer et al., 2004) in which glycine betaine analogs were synthesized, it was found that these analogs inhibited bacterial growth. In another study (Shneine et al., 2017) in which glycine derivatives were synthesized and their antibacterial effects were examined, glycine derivative (2S)-2-N-[(benzoyl-pyridin-2-yl-amino)-(4-Chloro-phenyl)-methyl]-L-alanine was found to be the most toxic against the gram-positive bacteria Staphylococcus aureus and the gram-negative bacteria Klebsiella pneumonia. In a study (Ajloo et al., 2015) in which palladium complexes of phenanthroline and glycine derivatives were synthesized, it is revealed that Pd (II) complexes bind to DNA by intercalation, consequently leading an increase in DNA's thermal stability and that the Pd (II) complex of methyl glycine exhibits a high toxicity against K562 leukemia cell line.

Though there are few studies on the physical properties (Wu et al., 2011) and use (Ni'mah & Woo, 2015; Wu et al., 2011) of glycine-based ionic liquids, no study on the biological activities of these ionic liquids is available in the literature.

There are not many studies on the biological activity of caprolactam which is the other starting material used to synthesize cluster CL-Gly. In few studies (Baxi, 2013; Iizuka et al., 1967), it has been notified that growth of some bacteria is inhibited in the presence of ε-caprolactam, whereas some bacteria use ε-caprolactam as a single source of carbon and nitrogen.

In this study; CL-Gly was synthesized and in order to understand its structure–activity relationship, the geometry optimization and molecular electrostatic potential and frontier molecular orbitals calculations were carried out using quantum-chemical calculations with density functional theory (DFT). Moreover, the antibacterial effects of the starting materials (caprolactam and glycine) and the cluster were investigated comparatively.

CONTACT Sefa Celik scelik@istanbul.edu.tr Physics Department, Science Faculty, Istanbul University, Vezneciler, Istanbul, 34134, Turkey.
Supplemental data for this article can be accessed online at https://doi.org/10.1080/07391102.2020.1748112.

2. Experimental and computational details

2.1. Synthesis

ε-Caprolactam (purity 99 wt%) and glycine (purity 99 wt%) were purchased from Aldrich and Merck, respectively.

ε-caprolactam (CL) – glycine (Gly) cluster (3) was prepared via a similar method to that (Moriel et al., 2010) in the literature: 149 mmol (Gly) (2) was added to an aqueous solution containing 12.4% by weight ε-caprolactam (123 mmol CL) (1) and the mixture was stirred at room temperature for 24 h.

After removing water at 60 °C under vacuum, 120 ml of acetonitrile and 40 ml of methanol were added to precipitate the unreacted amino acid, and the mixture was stirred vigorously overnight and then filtered. The purified cluster (3) was dried overnight at 60 °C and stored under moisture-free conditions. The formation reaction of the cluster is shown in Figure 1 (Celik et al., 2019).

The purity of the compound was checked by IR and Raman analysis. The ATR-FTIR and micro-Raman spectra of the synthesized cluster CL-Gly is given in comparison to those of solid caprolactam and Glycine in Figures 2 and 3, respectively. As seen in the figures, although CL-Gly cluster has CL and Gly vibrational bands, band wavenumber shifts were observed that indicative of CL and Gly interaction

2.2. Computational methods

The entire calculations in the present work are performed using the Gaussian 03 W (Frisch et al., 2004) program package on personal computer. The geometrical parameters are computed by optimizing the geometry of the molecule using DFT (Becke, 1993) method both b3lyp and wb97xd functionals with the 6-311++G(d,p) basis set. The both b3lyp and wb97xd functionals are used comparatively since the wb97xd (Chai & Head-Gordon, 2008a, 2008b) takes into account both short-range and long-range interactions, while b3lyp only takes into account short-range interactions. The optimized structures of CL-CL and CL-Gly and hydrogen bond lengths, calculated using DFT/b3lyp/6-311++G(d,p) and DFT/wb97xd/6-311++G(d,p) level of theories are given in Figure 4.

The harmonic force field of the cluster was evaluated via scaled quantum mechanical force field suggested by Pulay et al. (1983). Potential Energy Distributions of the cluster were computed by MOLVIB program (Sundius, 1990, 2002). Computed harmonic wavenumbers under 1800 cm^{-1} were multiplied by 0.98 and wavenumbers over 1800 cm^{-1} were multiplied by 0.96 (Balci & Akyuz, 2005). Calculated and scaled wavenumbers of CL-CL and CL-Gly were given in supporting information Table S1 in comparison with the experimental ATR-FTIR and Raman spectra of CL-Gly cluster.

2.3. Antibacterial activity

Antibacterial activity of the glycine, caprolactam and caprolactam-glycine were examined by disc diffusion method and agar dilution method according to clinical and laboratory standards institute (formerly CLSI) (CLSI, 2012).

The antibacterial activities were evaluated against Gram-positive (*Staphylococcus aureus* ATCC 29213, *Staphylococcus epidermidis* ATCC 12228, *Enterococcus faecalis* ATCC 29212, *Bacillus cereus* ATCC 11778, *Bacillus subtilis* ATCC 6633), Gram-negative (*E. coli* ATCC 25922, *Klebsiella pneumoniae* ATCC 4352, *Pseudomonas aeruginosa* ATCC 27853, *Salmonella enteritidis* KUEN 349, *Salmonella Typhimurium* ATCC 14028) bacteria. The strains were provided by the Faculty of Veterinary Medicine, Department of Microbiology Culture Collection, Istanbul University-Cerrahpasa. Mueller–Hinton Agar (Fluka 70191) was used for the detection of the qualitative and quantitative antibacterial effect and to maintain the strains. Mueller–Hinton broth (Fluka 90922) (CAMBH) with MgCl2·2H2O (10 mg Mg2+/L) and CaCl2·6H2O (20 mg Ca^{2+}/L) was used as the medium for dilution. Glycine, caprolactam and caprolactam-glycine were dissolved in DMSO at a concentration of 300 mg/ml, 500 mg/ml and 300 mg/ml respectively.

Disc diffusion method was used for screening the samples for the qualitative measurement of antibacterial activity. The Muller Hinton Agar plates were inoculated with 0.1 mL of 0,5 McFarland dilution of the tested culture. The discs (6 mm in diameter) were impregnated with 50 µl of the Gly, CL, CL-Gly and placed on the inoculated agar. The plates were incubated at 37 °C for 24 h. The plates were examined for possible clear zones after incubation. The presence of any clear zone that formed around the film on the plate medium was recorded as the growth inhibition zone against the microbial species. Gentamycin standard disc (10 µg) was placed onto agar plates for positive control. The tests were duplicated, and data were averaged.

For the detection of the antibacterial effect of the glycine, caprolactam and caprolactam-glycine quantitatively, the agar dilution method was performed. The components were prepared for two-fold step dilution for ten serial dilutions with CAMHB. 1 ml of each inoculum was poured to each petri dish, and 9 ml Muller-Hinton agar brought to 45–50 °C was added onto inoculum and mixed with a circular dial until at the room temperature. A bacterial suspension with 107 CFU/ml final concentration was prepared and was inserted into the microplate wells. The sterilised replicator with 3-mm pins, which deliver two µl, was placed into the microplate to soak the pins and transfer it onto the agar plate. The agars were incubated at 37 °C for 24 h. The minimum inhibitory concentration, MIC, the value was determined beyond the level no inhibition of growth of test organisms was observed. Furthermore, Gentamicin sulphate (Sigma G1272) was used as the antibiotic reference standard. The experiments were conducted twice, and data were averaged.

3. Results and discussion

Glycine, caprolactam and caprolactam-glycine were tested to determine their antibacterial activity against Gram-positive and negative bacteria through the disc diffusion method.

Caprolactam had the different level of antibacterial activity against four bacterial species, but it did not affect *E. faecalis*, *B. cereus*, *E. coli*, *K. pneumoniae*, *P. mirabilis*, *S. typhimirium*, and *S. enteritidis* species. The inhibition zones of the microorganisms sensitive to Caprolactam were 4–10 mm. The highest inhibition zone (10 mm) was observed against *P. aeruginosa*. The inhibition zone against *S. aureus* and *S. epidermidis* was

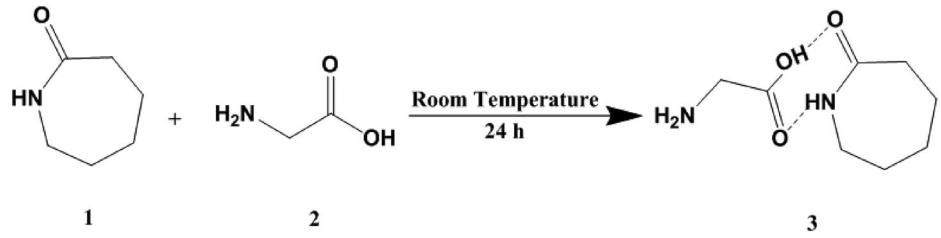

Figure 1. The reaction scheme of formation of CL-Gly cluster.

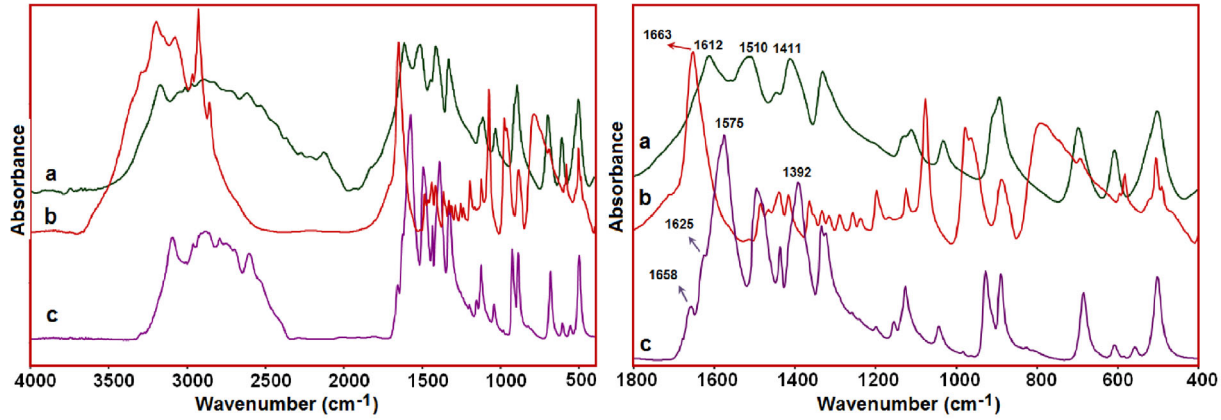

Figure 2. The ATR-FTIR spectra of Glycine (a), solid caprolactam (b) and CL-Gly (c).

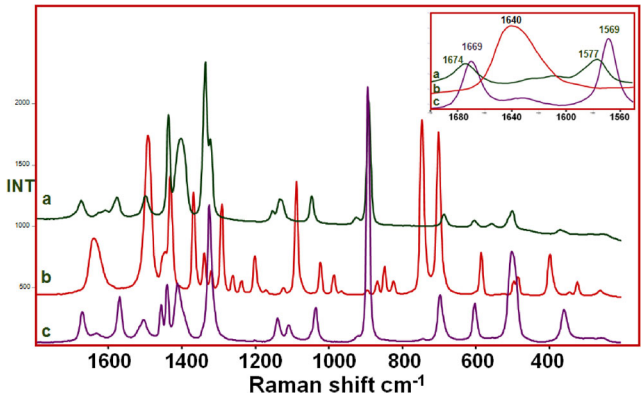

Figure 3. Micro-Raman spectra of Glycine (a), solid caprolactam (b) and CL-Gly (c). The enlarged 1700–1550 cm^{-1} region of the spectra is given in the upper frame.

8 mm while the component exhibited poor antibacterial activity against *B. subtilis* (4 mm) and there was no inhibition against rest of tested bacteria. The inhibition zones of the microorganisms sensitive to control antibiotic were 16–22 mm. The results obtained with caprolactam were determined to be incompatible with effects of control antibiotics.

Glycine and caprolactam-glycine did not form a measurable inhibition zone against any of the tested bacteria. The results of the disk diffusion test of components and positive control against 11 different bacterial species are shown in Table 1.

Glycine, caprolactam and caprolactam-glycine tested to determine their antibacterial activity against Gram-positive and negative bacteria through the agar dilution method. It was decided that the components have different levels of effect against bacterial species.

Glycine was found to affect both gram-positive and gram-negative bacteria. When evaluated against gram-positive bacteria, it was found to be effective against *S. epidermidis* and *B. subtilis* (MIC = 30 mg/ml), but no activity was seen against *S. aureus*, *E. faecalis* and *B. cereus*. The results obtained were determined to be incompatible with the effects of control antibiotics. When evaluated against gram-negative bacteria, it was found to be effective against *E. coli*, *K. pneumoniae*, *S. typhimirium* and *S. enteritidis* (MIC = 30 mg/ml). The component has not shown any antimicrobial activity against *P. aeruginosa* and *P. mirabilis*. The results were incompatible with results of control antibiotics.

It was determined that caprolactam have an effect on varying rates of bacteria except for *B. subtilis*. The caprolactam demonstrated the lowest MIC values against *S. aureus* and *S. epidermidis* (MIC = 6.25 mg/ml). It was found to be less effective against *E. faecalis* and *B. cereus* (MIC = 50 mg/ml). The highest effect was seen against *E. coli* and *P. aeruginosa* (MIC = 25 mg/ml) while it was found to be effective at MIC of 50 mg/ml against *S. pneumoniae*, *P. mirabilis*, *S. Typhimurium* and *S. enteritidis*. The results obtained were determined to be incompatible with the effects of control antibiotics.

CL-Gly has been shown activity in different levels on gram-positive and gram-negative bacteria. The component demonstrated the lowest MIC values against *B. subtilis* (MIC = 15mg/ml) and *S. epidermidis* (MIC = 30 mg/ml), while no activity was exhibited against *S. aureus*, *E. faecalis* and *B. cereus*. When evaluated against gram-negative bacteria, it was found to be effective against *E. coli*, *K. pneumoniae*, *S. typhimirium* and *S. enteritidis* at 30 mg/ml MIC value. The component has not shown any antimicrobial activity against *P. aeruginosa* and *P. mirabilis*. The results were incompatible with results of control antibiotics (Table 2).

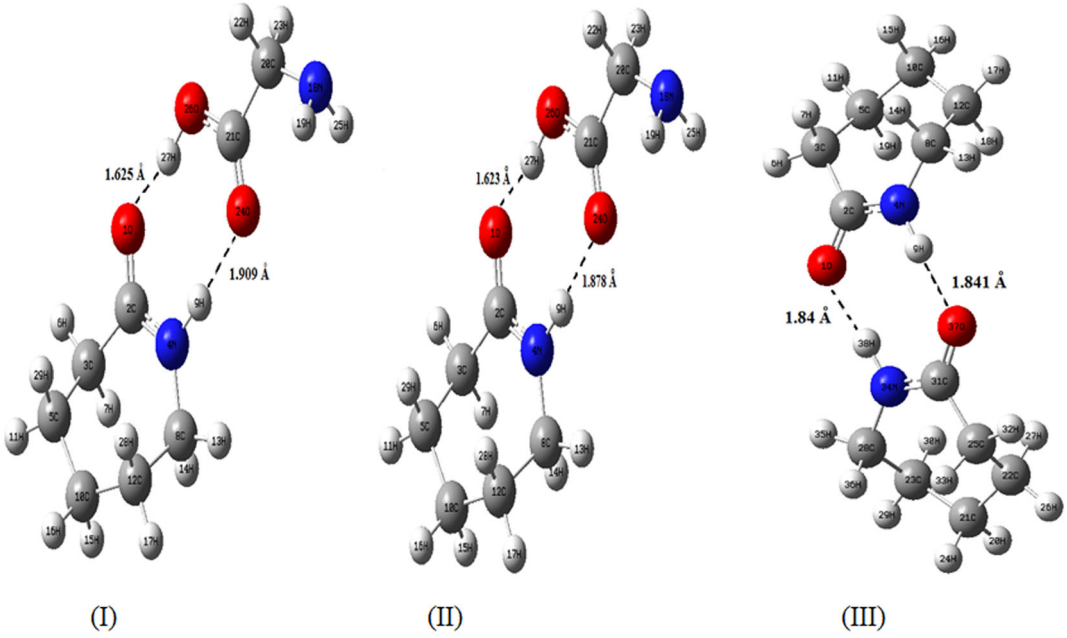

Figure 4. The optimized molecular structures of CL-Gly (I-II) and CL-CL(III) calculated using DFT/b3lyp/6-311++G(d,p) (I) and DFT/wb97xd/6-311++G(d,p) (II-III) level of theories.

Table 1. Results of the antibacterial activity of Gly, CL, CL-Gly by disc diffusion method.

		Diameter of inhibition zone (mm)			
Bacteria		Gly	CL	CL-Gly	Gentamicin
Gram positive bacteria	*S. aureus*	–	8	–	19
	S. epidermidis	–	8	–	20
	E. faecalis	–	–	–	
	B. cereus	–	–	–	22
	B. subtilis	–	4	–	18
Gram negative bacteria	*E. coli*	–	–	–	19
	K. pneumoniae	–	–	–	18
	P. aeruginosa	–	10	–	16
	P. mirabilis	–	–	–	18
	S. typhimirium	–	–	–	
	S. enteritidis	–	–	–	

3.1. Structure

The optimization of the new cluster examined reveals two strong hydrogen bonds between CL and Gly molecules; O1-H27 (1.623 Å) and O24-H9 (1.878 Å). The structural parameters of the optimized conformation of cluster are given in Table 3.

Dispersion correction contributed significantly to the interaction energy as shown in the study by Izgorodina et al. (2009). In this study, this correction was made in order to take into account the weak non-covalent interactions such as charge transfer interactions and van der Waals interactions. The interaction energy for (II) molecule $\{\Delta E = E_{CL\text{-}Gly} - (E_{CL} + E_{Gly})\}$ between CL and Gly are –20.8 kcal/mol (–0.901 eV), according to DFT/wb97xd functional theory.

3.2. Molecular electrostatic potential

The separation of the electric charge distribution in a molecule is explained by the polarity of a molecule. Thus, the centers of positive and negative charge distributions in the molecule cause a dipole moment. In order to explain the behavior of molecules during reactions and to understand where they bind to another molecule, MEP, which is calculated from the most stable (i.e. the lowest-energy) molecular geometries obtained using the DFT method at the wb97xd/6-311++ G(d,p) level of theory, is needed.

The centers of positive (the most electropositive) and negative (the most electronegative) charge distributions on the electrostatic potential surface of the cluster are represented by blue and red color, respectively (Figure 5). Magnitude of electrostatic potential represented by different colors is in the order: red with color code: -1.340 V < orange < yellow < green < blue with color code: $+1.340$ V.

Hydrogen atoms as positive potential regions pertaining to the NH and CH_2 groups are responsible for nucleophilic attack, while oxygen and nitrogen atoms as negative potential regions are responsible for electrophilic attack. These active sites show whether this cluster with a dipole moment of 4.79 D has a beneficial effect on the organism.

In a study on dipole moments of some ionic liquids (Studzińska et al., 2011), the dipole moments were found to be in the range of 1.91–17.31 D and our result is in good agreement with the previous findings.

3.3. Homo and LUMO energies

The highest molecular orbit occupied by electrons is called HOMO and the lowest molecular orbit occupied by electrons is called LUMO. HOMO functions as an electron donor because it is the outermost molecular orbit occupied by electrons, while LUMO functions as an electron acceptor since it is the first empty molecular orbit unoccupied by electrons. Thus, HOMO directly represents the ionisation potential of a molecule, while LUMO represents the electron affinity of the molecule. The energy gap between HOMO and LUMO is an indicator of the chemical stability of a molecule and is an

Table 2. Results of the antibacterial activity of Glycine, Caprolactam and Caprolactam-Glycine by agar dilution method.

		Minimum inhibitory concentrations (MIC) in mg/ml			
Bacteria		Gly	CL	CL-Gly	Gentamicin
Gram positive bacteria	*S. aureus*	Growth	6.25	Growth	0.002
	S. epidermidis	30	6.25	30	0.002
	E. faecalis	Growth	50	Growth	0.008
	B. cereus	Growth	50	Growth	0.002
	B. subtilis	30	Growth	15	0.002
Gram negative bacteria	*E. coli*	30	25	30	0.002
	K. pneumoniae	30	50	30	0.002
	P. aeruginosa	Growth	25	Growth	0.002
	P. mirabilis	Growth	50	Growth	0.002
	S. typhimirium	30	50	30	0.002
	S. enteritidis	30	50	30	0.002

Table 3. Structural parameters for monomeric form of new cluster obtained by DFT/B3LYP/(6-311++G(d,p)) (I) and DFT/wb97xd (6-311++G(d,p)) (II), in gas phase.

Atoms[a]	CL-Gly(I)	CL-Gly(II)	Atoms[a]	CL-Gly(I)	CL-Gly(II)	Atoms[a]	CL-Gly(I)	CL-Gly(II)
R(1,2)	1.243	1.238	R(18,25)	1.015	1.013	A(11,5,29)	106.2	106.3
R(1,27)	1.625	1.623	R(20,21)	1.526	1.521	A(4,8,12)	114.7	114.4
R(2,3)	1.517	1.513	R(20,22)	1.095	1.094	A(4,8,13)	105.7	105.9
R(2,4)	1.345	1.341	R(20,23)	1.094	1.094	A(4,8,14)	110.1	110.1
R(3,5)	1.543	1.537	R(21,24)	1.222	1.218	A(12,8,13)	109.5	109.5
R(3,6)	1.090	1.089	R(21,26)	1.321	1.312	A(12,8,14)	109.9	109.9
R(3,7)	1.097	1.097	R(26,27)	1.009	1.003	A(13,8,14)	106.5	106.6
R(4,8)	1.463	1.455	A(2,1,27)	127.9	127.6	A(4,9,24)	170.8	171.1
R(4,9)	1.023	1.022	A(1,2,3)	119.8	119.9	A(5,10,12)	115.5	115.2
R(5,10)	1.534	1.529	A(1,2,4)	121.5	121.6	A(5,10,15)	108.6	108.6
R(5,11)	1.094	1.094	A(3,2,4)	118.7	118.6	A(12,10,15)	108.7	108.7
R(5,29)	1.096	1.096	A(2,3,5)	114.3	113.9	A(12,10,16)	108.8	108.9
R(8,12)	1.534	1.529	A(2,3,6)	105.7	105.7	A(15,10,16)	106.1	106.2
R(8,13)	1.091	1.091	A(2,3,7)	109.3	109.3	A(8,12,10)	114.5	114.2
R(8,14)	1.097	1.097	A(5,3,6)	110.3	110.4	A(8,12,17)	107.8	107.9
R(9,24)	1.909	1.878	A(5,3,7)	109.6	109.6	A(8,12,28)	108.6	108.6
R(10,12)	1.534	1.529	A(6,3,7)	107.4	107.6	A(10,12,17)	108.5	108.5
R(10,15)	1.098	1.098	A(2,4,8)	126.9	126.6	A(10,12,28)	110.4	110.3
R(10,16)	1.095	1.094	A(2,4,9)	115.1	115.2	A(17,12,28)	106.7	106.9
R(12,17)	1.096	1.095	A(8,4,9)	117.9	118.3	A(19,18,20)	110.4	110.3
R(12,28)	1.096	1.096	A(3,5,10)	114.8	114.6	A(19,18,25)	106.1	106.1
R(18,19)	1.015	1.013	A(3,5,11)	107.8	107.9	A(20,18,25)	110.4	110.3
R(18,20)	1.451	1.445	A(3,5,29)	109.2	109.2	A(18,20,21)	116.5	116.2

[a]R and A stand for bond (Å), angle (degrees), respectively.

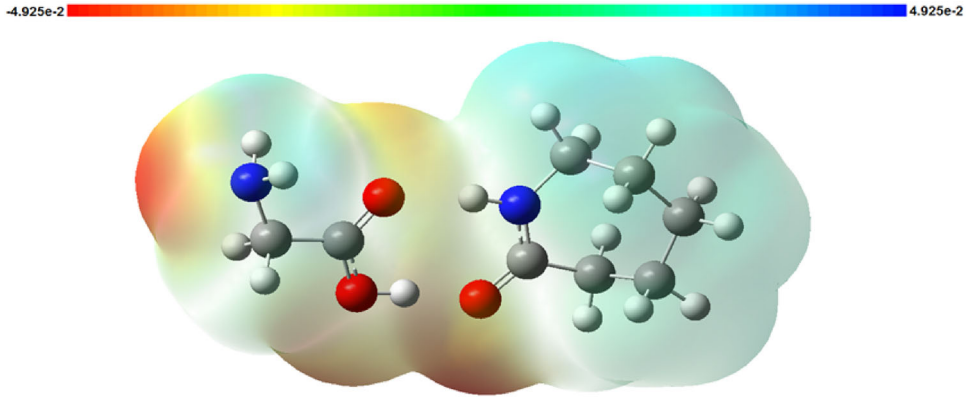

Figure 5. Molecular electrostatic potential (MEP) of CL-Gly obtained by DFT/wb97xd/6-311++G(d,p).

important parameter used to determine the flow properties of electrical charge of the molecule (Fukui, 1982; Koopmans, 1934). The LUMO molecular orbital is localized on caprolactam molecule, whereas the HOMO molecular orbital on the interaction zone of glycine and caprolactam molecules. The HOMO-LUMO energy range of the synthesized cluster was calculated and found to be 9.931 eV (Figure 6). In another study (Khan et al., 2014), this energy range for choline-based ionic liquid and its complexes was reported to be about 4–5.5 eV. The quantum chemical parameters such as ionization potential, the electron affinity, the electronegativity, the hardness and the electrophilicity, which describes the biological effect of the molecule, were calculated using Koopmans (1934) theorem and were found to be 8.979 eV, −0.952 eV, 4.0135 eV, 4.9655 eV and 1.622 eV, respectively.

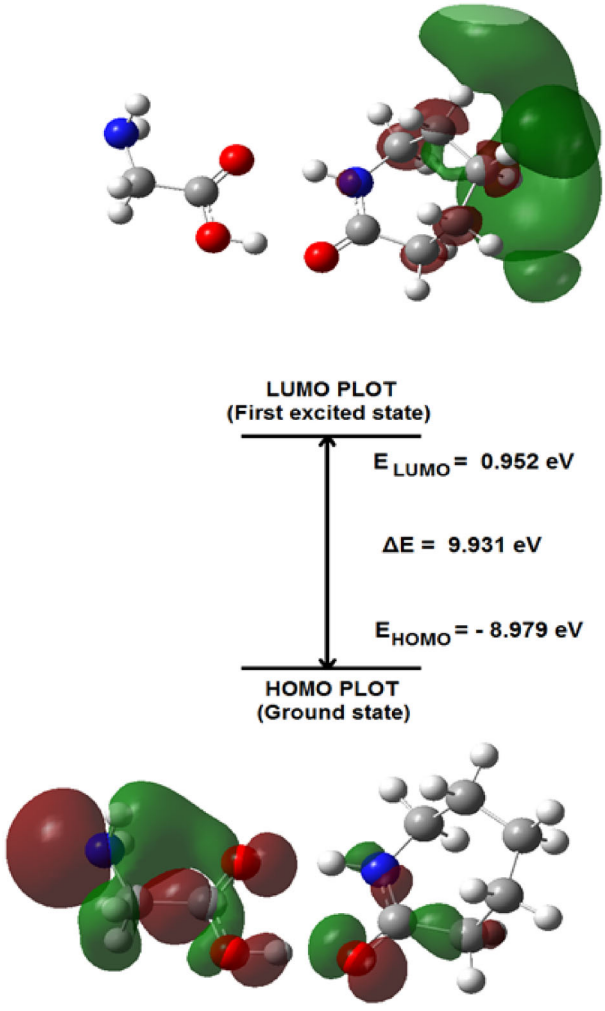

Figure 6. The atomic orbital HOMO-LUMO composition of the frontier molecular orbital for CL-Gly.

3.4. Docking studies

Molecular docking is a type of modeling that shows a stable three-dimensional structure consisting of interactions between two or more molecules and which bonds are formed between them.

Ionic liquids (ILs) have recently been used to dissolve biopolymers such as cellulose, elastin and chitin (Mantz et al., 2007; Swatloski et al., 2002) due to their high dissolving power (Dadi et al., 2007; Edgar et al., 2010; Tojo & Hirasawa, 2014) and also their dissolving degree can be adjusted by changing the cation and anion in their structure (Bulkowska et al., 2016). It has been reported that DNA, a natural biopolymer, can be stored at room temperature for a long time by maintaining its chemical and structural stability in 2-hydroxyethylammonium formate IL and dissolved at a high concentration in the IL (Singh et al., 2017). It has been demonstrated that this high dissolution and long-term stability is due to hydrogen bonds between the IL and DNA.

Autodock-Vina program (Trott & Olson, 2009) was used to show the region in which any binding between CL-Gly IL and DNA takes place and the interaction between CL and Gly. The three dimensional molecular structure of DNA was obtained from the protein data bank (PDB ID: 1BNA) (Drew et al., 1981) DNA was made suitable to the docking by removing water molecules in DNA and adding polar hydrogens in it and the Kollman charges of DNA were determined. After optimization of CL-Gly molecule in gas phase for adapting the docking, Geistenger method was used to find the partial charges of the synthesized molecule. The active site of DNA which was defined within the grid size of 40 × 40 x 40 Å was bound to the CL-Gly molecule by hydrogen bonds (Figure 7). The stable CL-Gly structure in DFT/wb97xd/6-311++G(d,p) level of theory is bound to the DT8, DG10, DG16 and DA17 residues of DNA via the hydrogen bonds. There are H-bonding interactions between the DG16, DA17 residues of DNA and the carbonyl oxygen of caprolactam molecule and also between the DT8, DG10 residues and hydrogen/oxygen atom in Gly molecule.

Since a stable complex is formed between the DNA and CL-Gly IL, it can be concluded that the stability of the DNA is improved. Using UCSF Chimera program (Pettersen et al., 2004) and, TIP3PBOX solvent model for which simulation time of the IL solvated in a cubic box with 921 water molecules was 1.2 ns (120 10^3 frames), CL-Gly IL was simulated at the molecular level. Since the clusters had problems in performing MD simulations, the hydrogen bond lengths between Gly and CL were kept constant. The stable conformations of ligand can be clearly seen from RMSD graphs (supporting information Figure S1). Following the use of MD simulation results for re-docking of CL-Gly with DNA, it is remarkable that the lowest-energy conformer (–6.8 kcal/mol) determined by MD simulations is numerically very close to that obtained by optimized geometries (–6.7 kcal/mol). It follows from the obtained docking model that the nucleobases DC9, DG10, DC11, DG16, DA17 and DA18 of DNA receptor interacted with CL-Gly (supporting information Figure S2). Quantum mechanical calculation rendered possible to find the optimized geometry. In consequence of docking analysis using the optimized geometry, the active sites of the DNA receptor to bind were shown to be DG10, DG16 and DA17, which infers that the results obtained in both calculations confirmed each other.

In some studies carried out with different ligands over the past decade, it has been shown that especially the nucleobase DG10 of DNA is active site to bind (Allaka et al., 2018; Cheraghi et al., 2017; Das et al., 2018; Vijayalakshmi et al., 2013, 2014).

3.5. Analysis of toxicological and physicochemical properties

Toxic risk assessment is a criterion that indicates whether a chemical has a toxic effect (i.e. a potential health risk) on the organism. Toxic risk assessment comprises the following factors: hazard identification, dose-response assessment, exposure assessment, and risk characterization (Pepper et al., 2015).

The partition coefficient (P) is the ratio of the concentration of a compound in octanol as a non-polar solvent to its concentration in water as a polar solvent, thus being an indication of the hydrophilicity of a compound and it is

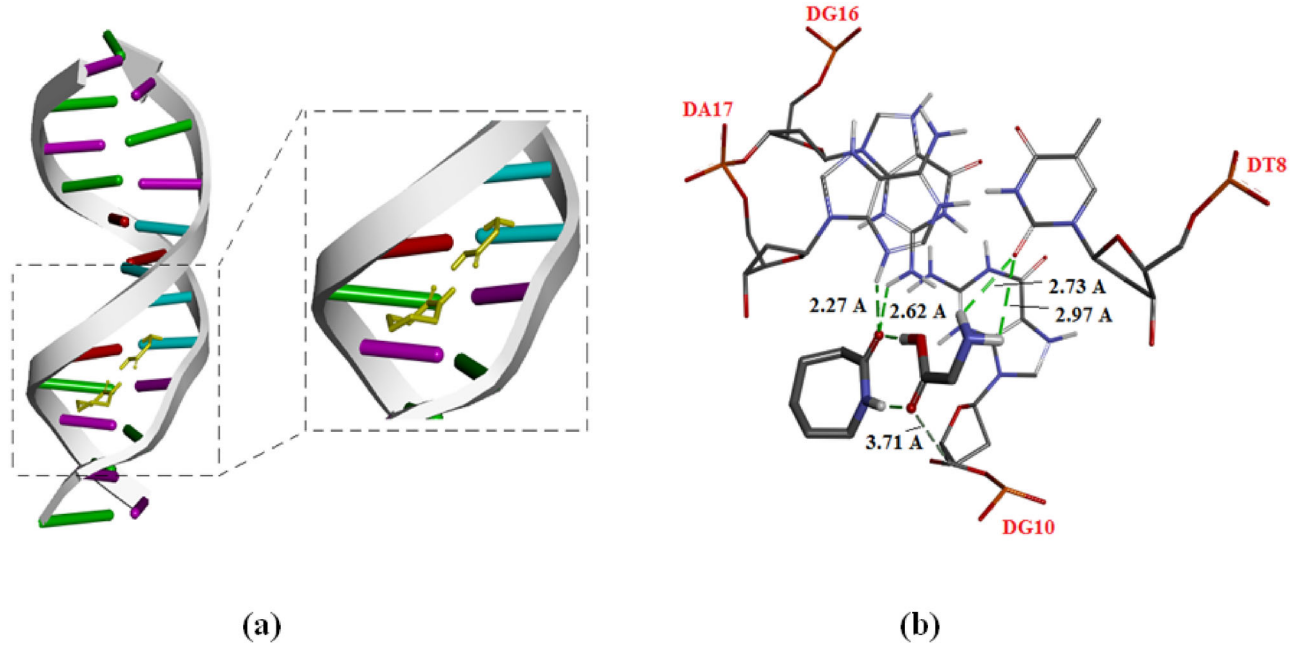

Figure 7. (a) Docking of CL-Gly with DNA. (b) The dotted lines present the interactions (binding affinity −6.7 kcal/mol).

represented by clogP as the logarithm of the partition coefficient. The lower the logP value of a drug, the more hydrophilic it is (Van de Waterbeemd et al., 2001), thus making it slower to be absorbed orally (Qiu et al., 2017).

The solubility of a compound in water is indicated by logS and is a measure of absorption. the greater the logS, the higher the absorption (Ishikawa & Hashimoto, 2011). As the molecular weight of the compounds increases, their polarity decreases further and their solubility in water decreases (Faust & Aly, 1998). Water-soluble drugs are less soluble in lipid (Meisenberg & Simmons, 2016).

The topological polar surface area (TPSA), defined as the surface sum on electronegative atoms in a molecule, is another absorption criterion for evaluating pharmacokinetics (for instance, intestinal absorption, Caco-2 monolayer penetration, blood-brain barrier penetration) (Ertl et al., 2000). The higher the TPSA of a compound, the more difficult it is to penetrate through the cell membrane (Begley, 2008). When TPSA is greater than 140 $Å^2$ and molecular weight is greater than 500 g, human intestinal absorption is restricted (Brito, 2011; Di & Kerns, 2015).

Drug score refers to the potential for a molecule to be used as a drug depending on druglikeness, clogP, logS, molecular weight and toxicity risks (Krishna et al., 2012). A positive and high drug score toward 1 indicates that molecule has a drug-like structure and usability as a drug, whereas a drug score approaching 0 indicates a high risk for that molecule to use as a drug (Guan et al., 2019). However, it is necessary to investigate the effects of the compound in vivo to confirm its usability as a drug (Hosoya & Czysz, 2016).

The estimated values of the toxicity risks of CL (Celik et al., 2020) was calculated in our previous study. The estimated values of the toxicity risks of Gly and Cl-Gly IL together with some important physicochemical properties were determined using OSIRIS Property Explorer (OSIRIS, 2010) and Molsoft (https://www.molsoft.com/mprop/). The results are given in Table 4.

3.6. Absorption analysis of target cluster

Blood brain barrier (BBB) formed by endothelial cells (Ballabh et al., 2004) protects the central nervous system by limiting the passage of neurotherapeutics and small-molecule drugs into the brain (Greene & Campbell, 2016). Drugs with CNS activity can only have an action in brain by passing through blood-brain barrier (Patrick, 2013). The more hydrophobic the drug is, the higher the transport to the brain (Mutschler & Derendorf, 1995).

BBB permeable (+) is an essential concept that protects peripheral organs (central nervous system) against neurotoxins and governs and regulates the diffusion of drugs through blood-brain barrier (Erdő et al., 2017).

Small intestine is an organ with large surface area (Helander & Fandriks, 2014) which carries out the absorption of oral drugs to enable them to enter the bloodstream. Drugs taken orally are mainly absorbed by the intestines (Murakami, 2017). Intestinal absorption is of great importance for the rapid absorption of drugs, hence in terms of improving bioavailability (Peterson et al., 2019). The absorption percentages of the compounds having poor apparent permeability (poor absorption), medium permeability (mid-level absorption) and high permeability (strong absorption) coefficients range from 0 to 20%, 20 to 70% and 70 to 100%, respectively (Yee, 1997).

Caco-2 (human colon epithelial cancer cell line, model of the intestinal epithelial barrier) is an assay dealing with intestinal absorption to evaluate the permeability of drugs (Van Breemen & Li, 2005).

P-glycoprotein (P-gp), which is available in epithelial cells and also the endothelial cells (You et al., 2014), is an efflux drug transporter that serves as a biological barrier that

Table 4. Prediction of toxicity risks and physicochemical properties by Osiris and Molsoft of title compounds.

	Toxicity risks				Physicochemical properties					
Compound	Mutagenic	Tumorigenic	Irritant	Reproductive Effect	CLogP	Solubility	MW	TPSA	Drug likeness	Drugscore
CL (Celik et al., 2020)	(+)	(+)	(+)	(+)	0.52	−1.38	113	29.1	−7.96	0.06
Gly	(+)	(−)	(−)	(−)	−3.35	−0.03	75	63.32	−1.67	0.35
CL-Gly					−0.88	−0.97	188.12	76.55	−1.54	

Table 5. Prediction of ADMET profiles of the CL-Gly.

ADMET predicted profile: classification		
Model	Result	Probability
Absorption		
Blood-brain barrier	BBB+	0.8460
Human Intestinal Absorption	HIA-	0.5000
Caco-2 permeability	Caco2-	0.7677
P-glycoprotein substrate	Substrate	0.5836
P-glycoprotein inhibitor	Non-inhibitor	0.9595
	Non-inhibitor	0.9926
Renal organic cation transporter	Non-inhibitor	0.8847
Distribution		
Subcellular localization	Mitochondria	0.6911
Metabolism		
CYP450 2C9 substrate	Non-substrate	0.8799
CYP450 2D6 substrate	Non-substrate	0.7824
CYP450 3A4 substrate	Non-substrate	0.7221
CYP450 1A2 inhibitor	Non-inhibitor	0.9416
CYP450 2C9 inhibitor	Non-inhibitor	0.9676
CYP450 2D6 inhibitor	Non-inhibitor	0.9613
CYP450 2C19 inhibitor	Non-inhibitor	0.9454
CYP450 3A4 inhibitor	Non-inhibitor	0.9556
CYP inhibitory promiscuity	Low CYP inhibitory promiscuity	1.0000
Excretion		
Toxicity		
Human ether-a-go-go-related gene inhibition	Weak inhibitor	0.9910
	Non-inhibitor	0.8988
AMES toxicity	Non AMES toxic	0.8309
Carcinogens	Non-carcinogens	0.9623
Fish toxicity	Low FHMT	0.9416
Tetrahymena pyriformis toxicity	Low TPT	0.9598
Honey bee toxicity	Low HBT	0.8054
Biodegradation	Ready biodegradable	0.5000
Acute oral toxicity	III	0.6531
Carcinogenicity (three-class)	Non-required	0.6672
ADMET predicted profile: regression	**Value**	**Unit**
Absorption		
Aqueous solubility	−1.8796	LogS
Caco-2 permeability	0.1483	LogPapp, cm/s
Distribution		
Metabolism		
Excretion		
Toxicity		
Rat acute toxicity	1.8099	LD50, mol/kg
Fish toxicity	2.7847	pLC50, mg/L
Tetrahymena pyriformis toxicity	−0.7429	pIGC50, ug/L

protects cells from the harmful effects of drugs by transporting toxins and xenobiotics out of cells (Brunton et al., 2010). Consequently, it ensures that hazardous substances on human health are excreted through gastrointestinal tract, bile and urine (Amin, 2013).

Cytochrome P450 is a hemeprotein that metabolizes exogenous and endogenous compounds that are toxic to cells (Yahia, 2018).

Potassium (K +) channels found in cell membranes allow potassium ions to flow into and out of the cell (Waxman, 2005), thereby modulating the electrical properties of the cells (Yasuda et al., 2008).

The various ADMET parameters of the investigated cluster, are characterized using the silico module admetSAR (Cheng et al., 2012). The predicted values of CL-Gly are given in Table 5.

The BBB is the microvascular endothelial cell layer of the brain and plays an important role in separating the brain from the blood. The BBB permeability is required for the central nervous system drugs, whereas for the non-central nervous system drugs the BBB penetration should be minimized, to avoid undesired side effect. According to the predicted properties, the investigated IL is found to be BBB permeable (BBB+). The drug permeability in human

intestinal epithelial (Caco-2) cells is used to control intestinal absorption. It is an in vitro model used to predict drug absorption in which the drug is administered orally. From Caco2 permeability study it was observed that IL has a negative result in Caco2 permeability, indicating that it was not permeable. Human intestinal absorption, HIA, as a key procedure of oral absorption, unfortunately, the investigated IL has a negative results in HIA.

4. Conclusions

In this study molecular structure, electronic properties and the antibacterial activities of new synthesized cluster CL-Gly were evaluated. It has been shown that CL-Gly has antibacterial activity in different levels on gram-positive and gram-negative bacteria. The interaction between DNA and CL-Gly was achieved by molecular docking study. It was found that CL-Gly made a stable complex with DNA, thus can be used for DNA stabilization. In silico ADMET study was also performed for predicting pharmacokinetic and toxicity profile of the synthesized cluster which expressed good drug-like behavior and non-toxic nature. It was revealed that the compound has a potential to become an important molecule in drug discovery process.

Disclosure statement

No potential conflict of interest was reported by the authors.

Funding

This study was supported by the Research funds of Istanbul University [ÖNAP-2423], [N-3341], [N-3875].

References

Ajloo, D., Moghadam, M. E., Ghadimi, K., Ghadamgahi, M., Saboury, A. A., Divsalar, A., SheikhMohammadi, M., & Yousefi, K. (2015). Synthesis, characterization, spectroscopy, cytotoxic activity and molecular dynamic study on the interaction of three palladium complexes of phenanthroline and glycine derivatives with calf thymus DNA. *Inorganica Chimica Acta*, *430*, 144–160. doi:10.1016/j.ica.2015.03.006

Allaka, T. R., Katari, N. K., Veeramreddy, V., & Anireddy, J. S. (2018). Molecular modeling studies of novel fluoroquinolone molecules. *Current Drug Discovery Technologies*, *15*(2), 109–122. doi:10.2174/1570163814666170829142044

Amin, M. L. (2013). P-glycoprotein inhibition for optimal drug delivery. *Drug Target Insights*, *7*, DTI.S12519. doi:10.4137/DTI.S12519

Atkinson, J., & Hibert, C. (2001). *Chemistry*. Heinemann.

Balci, K., & Akyuz, S. (2005). A theoretical vibrational spectroscopic study with density functional theory and force field refinement calculation methods on free 4-aminopyrimidine molecule. *Journal of Molecular Structure*, *744-747*, 909–919. doi:10.1016/j.molstruc.2004.10.099

Ballabh, P., Braun, A., & Nedergaard, M. (2004). The blood–brain barrier: An overview: Structure, regulation, and clinical implications. *Neurobiology of Disease*, *16*(1), 1–13. doi:10.1016/j.nbd.2003.12.016

Baxi, N. N. (2013). Influence of ε-caprolactam on growth and physiology of environmental bacteria. *Annals of Microbiology*, *63*(4), 1471–1476. doi:10.1007/s13213-013-0610-4

Becke, A. D. (1993). Density functional thermochemistry. III. The role of exact exchange. *Journal of Chemical Physics*, *98*(7), 5648–5652. doi:10.1063/1.464913

Begley, T. P. (2008). *Wiley encyclopedia of chemical biology* (Vol. 1). Wiley.

Bontenbal, E., & de Bert, T. V. (2006). U.S. Patent Application No. 11/211,755.

Brito, M. A. D. (2011). Pharmacokinetic study with computational tools in the medicinal chemistry course. *Brazilian Journal of Pharmaceutical Sciences*, *47*(4), 797–805. doi:10.1590/S1984-82502011000400017

Brunton, L. L., Chabner, B. A., & Knollmann, B. C. (2010). *Goodman & Gilman's the pharmacological basis of therapeutics* (12th ed.). McGraw-Hill Professional.

Bulkowska, K., Gusiatin, Z. M., Klimiuk, E., Pawlowski, A., & Pokoj, T. (Eds.). (2016). *Biomass for biofuels*. CRC Press.

Celik, S., Albayrak, A. T., Akyuz, S., & Ozel, A. E. (2020). Synthesis, molecular docking and ADMET study of ionic liquid as anticancer inhibitors of DNA and COX-2, TOPII enzymes. *Journal of Biomolecular Structure and Dynamics*, *38*(5), 1311–1354. doi:10.1080/07391102.2019.1604263

Celik, S., Ozel, A. E., Akyuz, S., Albayrak, A. T., & Sigirci, B. D. (2019). Antibakteriyel aktiviteye sahip kaprolaktam-glisin iyonik sıvısı, moleküler modellemesi ve kullanımları, Patent Application No. TR 2019/00595, Turkey.

Chai, J. D., & Head-Gordon, M. (2008a). Long-range corrected hybrid density functionals with damped atom–atom dispersion corrections. *Physical Chemistry Chemical Physics*, *10*(44), 6615–6620. doi:10.1039/b810189b

Chai, J. D., & Head-Gordon, M. (2008b). Systematic optimization of long-range corrected hybrid density functionals. *The Journal of Chemical Physics*, *128*(8), 084106. doi:10.1063/1.2834918

Cheng, F., Li, W., Zhou, Y., Shen, J., Wu, Z., Liu, G., Lee, P. W., & Tang, Y. (2012). admetSAR: A comprehensive source and free tool for evaluating chemical ADMET properties. *Journal of Chemical Information and Modeling*, *52*(11), 3099–3105. doi:10.1021/ci300367a

Cheraghi, S., Taher, M. A., Karimi-Maleh, H., & Faghih-Mirzaei, E. (2017). A nanostructure label-free DNA biosensor for ciprofloxacin analysis as a chemotherapeutic agent: An experimental and theoretical investigation. *New Journal of Chemistry*, *41*(12), 4985–4989. doi:10.1039/C7NJ00609H

CLSI. (2012). *Methods for dilution antimicrobial susceptibility tests for bacteria that grow aerobically; approved standard – M07-A9* (9th ed.). Clinical and Laboratory Standards Institute.

Cosquer, A., Ficamos, M., Jebbar, M., Corbel, J. C., Choquet, G., Fontenelle, C., Uriac, P., & Bernard, T. (2004). Antibacterial activity of glycine betaine analogues: Involvement of osmoporters. *Bioorganic & Medicinal Chemistry Letters*, *14*(9), 2061–2065. doi:10.1016/j.bmcl.2004.02.045

Dadi, A. P., Schall, C. A., & Varanasi, S. (2007). Mitigation of cellulose recalcitrance to enzymatic hydrolysis by ionic liquid pretreatment. *Applied Biochemistry and Biotechnology*, *137–140*(1–12), 407–421. doi:10.1007/s12010-007-9068-9

Das, S., da Silva, C. J., Silva, M. d M., Dantas, M. D. d A., de Fátima, Â., Góis Ruiz, A. L. T., da Silva, C. M., de Carvalho, J. E., Santos, J. C. C., Figueiredo, I. M., da Silva-Júnior, E. F., de Aquino, T. M., de Araújo-Júnior, J. X., Brahmachari, G., & Modolo, L. V. (2018). Highly functionalized piperidines: Free radical scavenging, anticancer activity, DNA interaction and correlation with biological activity. *Journal of Advanced Research*, *9*, 51–61. doi:10.1016/j.jare.2017.10.010

Di, L., & Kerns, E. H. (Eds.). (2015). *Blood-brain barrier in drug discovery: Optimizing brain exposure of CNS drugs and minimizing brain side effects for peripheral drugs*. John Wiley & Sons.

Drew, H. R., Wing, R. M., Takano, T., Broka, C., Tanaka, S., Itakura, K., & Dickerson, R. E. (1981). Structure of a B-DNA dodecamer: Conformation and dynamics. *Proceedings of the National Academy of Sciences of the United States of America*, *78*(4), 2179–2183.

Edgar, K. J., Heinze, T., & Buchanan, C. M. (Eds.). (2010). *Polysaccharide materials: Performance by design*. American Chemical Society.

Erdő, F., Denes, L., & de Lange, E. (2017). Age-associated physiological and pathological changes at the blood–brain barrier: A review. *Journal of Cerebral Blood Flow & Metabolism*, *37*(1), 4–24. doi:10.1177/0271678X16679420

Ertl, P., Rohde, B., & Selzer, P. (2000). Fast calculation of molecular polar surface area as a sum of fragment-based contributions and its application to the prediction of drug transport properties. *Journal of Medicinal Chemistry*, *43*(20), 3714–3717. doi:10.1021/jm000942e

Faust, S. D., & Aly, O. M. (1998). *Chemistry of water treatment*. CRC Press.

Frisch, M. J., Trucks, G. W., Schlegel, H. B., Scuseria, G. E., Robb, M. A., Cheeseman, J. R., Montgomery, Jr., J. A., Vreven, T., Kudin, K. N., Burant, J. C., Millam, J. M., Iyengar, S. S., Tomasi, J., Barone, V., Mennucci, B., Cossi, M., Scalmani, G., Rega, N., Petersson, G. A., … Pople, J. A. (2004). *Gaussian 03, Revision C. 02*. Gaussian, Inc.

Fukui, K. (1982). Role of frontier orbitals in chemical reactions. *Science*, *218*(4574), 747–754. doi:10.1126/science.218.4574.747

Greene, C., & Campbell, M. (2016). Tight junction modulation of the blood brain barrier: CNS delivery of small molecules. *Tissue Barriers*, *4* (1), e1138017. doi:10.1080/21688370.2015.1138017

Guan, L., Yang, H., Cai, Y., Sun, L., Di, P., Li, W., Liu, G., & Tang, Y. (2019). ADMET-score-a comprehensive scoring function for evaluation of chemical drug-likeness. *MedChemComm*, *10*(1), 148–157.

Helander, H. F., & Fandriks, L. (2014). Surface area of the digestive tract–revisited. *Scandinavian Journal of Gastroenterology*, *49*(6), 681–689. doi:10.3109/00365521.2014.898326

Hosoya, M., & Czysz, K. (2016). Translational prospects and challenges in human induced pluripotent stem cell research in drug discovery. *Cells*, *5*(4), 46. doi:10.3390/cells5040046

Iizuka, H., Tanabe, I., Fukumura, T., & Kato, K. (1967). Taxonomic study on the ε-caprolactam-utilizing bacteria. *The Journal of General and Applied Microbiology*, *13*(2), 125–137. doi:10.2323/jgam.13.125

Ishikawa, M., & Hashimoto, Y. (2011). Improvement in aqueous solubility in small molecule drug discovery programs by disruption of molecular planarity and symmetry. *Journal of Medicinal Chemistry*, *54*(6), 1539–1554. doi:10.1021/jm101356p

Izgorodina, E. I., Bernard, U. L., & MacFarlane, D. R. (2009). Ion-pair binding energies of ionic liquids: Can DFT compete with ab initio-based methods? *The Journal of Physical Chemistry A*, *113*(25), 7064–7072. doi:10.1021/jp8107649

Khan, I., Kurnia, K. A., Sintra, T. E., Saraiva, J. A., Pinho, S. P., & Coutinho, J. A. (2014). Assessing the activity coefficients of water in cholinium-based ionic liquids: Experimental measurements and COSMO-RS modeling. *Fluid Phase Equilibria*, *361*, 16–22. doi:10.1016/j.fluid.2013.10.032

Koopmans, T. A. (1934). Ordering of wave functions and eigenvalues to the individual electrons of an atom. *Physica*, *1*(1–6), 104–113.

Krishna, P. V., Babu, M. R., & Ariwa, E. (Eds.). (2012). Global trends in computing and communication systems. 4th International Conference, Vellore, TN, India. OBCOM 2011 December 9–11, 2011, Part I. Proceedings (Vol. 269). Springer.

Lee, W. W., Kim, W. S., Ahn, G., Kim, K. N., Heo, S. J., Cho, M., Fernando, I. P. S., Kang, N., & Jeon, Y. J. (2016). Separation of glycine-rich proteins from sea hare eggs and their anti-cancer activity against U937 leukemia cell line. *EXCLI Journal*, *15*, 329.

Mahmoud, W. H., Mohamed, G. G., & El-Dessouky, M. M. (2015). Synthesis, structural characterization, in vitro antimicrobial and anticancer activity studies of ternary metal complexes containing glycine amino acid and the anti-inflammatory drug lornoxicam. *Journal of Molecular Structure*, *1082*, 12–22. doi:10.1016/j.molstruc.2014.10.014

Mantz, R. A., Fox, D. M., Green, J. M., Fylstra, P. A., De Long, H. C., & Trulove, P. C. (2007). Dissolution of biopolymers using ionic liquids. *Zeitschrift Fur Naturforschung A*, *62*(5–6), 275–280.

Meisenberg, G., & Simmons, W. H. (2016). *Principles of medical biochemistry e-book*. Elsevier Health Sciences.

Minami, M., Ando, T., Hashikawa, S. N., Torii, K., Hasegawa, T., Israel, D. A., Ina, K., Kusugami, K., Goto, H., & Ohta, M. (2004). Effect of glycine on Helicobacter pylori in vitro. *Antimicrobial Agents and Chemotherapy*, *48*(10), 3782–3788. doi:10.1128/AAC.48.10.3782-3788.2004

Moriel, P., Garcia-Suarez, E. J., Martinez, M., Garcia, A. B., Montes-Moran, M. A., Calvino-Casilda, V., & Banares, M. A. (2010). Synthesis, characterization, and catalytic activity of ionic liquids based on biosources. *Tetrahedron Letters*, *51*(37), 4877–4881. doi:10.1016/j.tetlet.2010.07.060

Murakami, T. (2017). Absorption sites of orally administered drugs in the small intestine. *Expert Opinion on Drug Discovery*, *12*(12), 1219–1232. doi:10.1080/17460441.2017.1378176

Mutschler, E., & Derendorf, H. (1995). *Drug actions: Basic principles and therapeutic aspects*. CRC press.

Ni'mah, H., & Woo, E. M. (2015). Effects of Glycine-Based Ionic Liquid on Spherulite Morphology of Poly (l-Lactide). *Macromolecular Chemistry and Physics*, *216*(12), 1291–1301. doi:10.1002/macp.201500046

OSIRIS. (2010). OSIRIS Property Explorer. Actelion Pharmaceuticals Ltd. Retrieved from http://www.organic-chemistry.org/prog/peo/

Oxtoby, D. W., Gillis, H. P., & Campion, A. (2011). *Principles of modern chemistry*. Cengage Learning.

Patrick, G. L. (2013). *An introduction to medicinal chemistry*. Oxford Iniversity Press.

Pepper, I. L., Gerba, C. P., & Gentry, T. J. (2015). *Environmental microbiology*. Academic Press.

Peterson, B., Weyers, M., Steenekamp, J. H., Steyn, J. D., Gouws, C., & Hamman, J. H. (2019). Drug bioavailability enhancing agents of natural origin (bioenhancers) that modulate drug membrane permeation and pre-systemic metabolism. *Pharmaceutics*, *11*(1), 33. doi:10.3390/pharmaceutics11010033

Pettersen, E. F., Goddard, T. D., Huang, C. C., Couch, G. S., Greenblatt, D. M., Meng, E. C., & Ferrin, T. E. (2004). UCSF Chimera—A visualization system for exploratory research and analysis. *Journal of Computational Chemistry*, *25*(13), 1605–1612. doi:10.1002/jcc.20084

Pulay, P., Fogarasi, G., Pongor, G., Boggs, J. E., & Vargha, A. (1983). Combination of theoretical ab initio and experimental information to obtain reliable harmonic force constants. Scaled quantum mechanical (SQM) force fields for glyoxal, acrolein, butadiene, formaldehyde, and ethylene. *Journal of the American Chemical Society*, *105*(24), 7037–7047.

Qiu, Y., Chen, Y., Zhang, G. G., Yu, L., & Mantri, R. V. (Eds.). (2017). *Developing solid oral dosage forms: Pharmaceutical theory and practice*. Academic Press.

Roesler, B. M. (2016). Extradigestive manifestations of helicobacter pylori infection: An overview. Published by ExLi4EvA.

Sepahi, M., Jalal, R., & Mashreghi, M. (2017). Antibacterial activity of poly-l-arginine under different conditions. *Iranian Journal of Microbiology*, *9*(2), 103.

Shneine, J. K., Qassem, D. Z., & Mahmoud, S. S. (2017). Synthesis, characterization and antibacterial activity of some aminoacid derivatives. *International Journal of ChemTech Research*, *10*(3), 604–612.

Singh, N., Sharma, M., Mondal, D., Pereira, M. M., & Prasad, K. (2017). Very high concentration solubility and long-term stability of DNA in an ammonium-based ionic liquid: A suitable medium for nucleic acid packaging and preservation. *ACS Sustainable Chemistry & Engineering*, *5*(2), 1998–2005. doi:10.1021/acssuschemeng.6b02842

Studzińska, S., Molíková, M., Kosobucki, P., Jandera, P., & Buszewski, B. (2011). Study of the interactions of ionic liquids in IC by QSRR. *Chromatographia*, *73*(S1), 35–44. doi:10.1007/s10337-011-1960-3

Sundius, T. (1990). MOLVIB: A program for harmonic force field calculations, QCPE program. *Journal of Molecular Structure*, *218*(604), 321–326. doi:10.1016/0022-2860(90)80287-T

Sundius, T. (2002). Scaling of ab initio force fields by MOLVIB. *Vibrational Spectroscopy*, *29*(1-2), 89–95. doi:10.1016/S0924-2031(01)00189-8

Swatloski, R. P., Spear, S. K., Holbrey, J. D., & Rogers, R. D. (2002). Dissolution of cellulose [correction of cellose] with ionic liquids. *Journal of the American Chemical Society*, *124*(18), 4974–4975. doi:10.1021/ja025790m

Tojo, S., & Hirasawa, T. (2014). *Research approaches to sustainable biomass systems*. Academic Press.

Trott, O., & Olson, A. J. (2009). AutoDock Vina: Improving the speed and accuracy of docking with a new scoring function, efficient optimization, and multithreading. *Journal of Computational Chemistry*, *31*(2), NA–461. doi:10.1002/jcc.21334

Van Breemen, R. B., & Li, Y. (2005). Caco-2 cell permeability assays to measure drug absorption. *Expert Opinion on Drug Metabolism & Toxicology*, *1*(2), 175–185. doi:10.1517/17425255.1.2.175

Van de Waterbeemd, H., Folkers, G., & Guy, R. (Eds.). (2001). *Pharmacokinetic optimization in drug research: Biological, physicochemical, and computational strategies*. John Wiley & Sons.

Vijayalakshmi, P., Selvaraj, C., Shafreen, R. M. B., Singh, S. K., Pandian, S. K., & Daisy, P. (2014). Ligand-based pharmacophore modelling and screening of DNA minor groove binders targeting Staphylococcus aureus. *Journal of Molecular Recognition*, *27*(7), 429–437. doi:10.1002/jmr.2363

Vijayalakshmi, P., Selvaraj, C., Singh, S. K., Nisha, J., Saipriya, K., & Daisy, P. (2013). Exploration of the binding of DNA binding ligands to Staphylococcal DNA through QM/MM docking and molecular dynamics simulation. *Journal of Biomolecular Structure and Dynamics*, *31*(6), 561–571. doi:10.1080/07391102.2012.706080

Waxman, S. (2005). *Multiple sclerosis as a neuronal disease*. Elsevier.

Wu, T. Y., Chen, B. K., Hao, L., Lin, Y. C., Wang, H. P., Kuo, C. W., & Sun, I. W. (2011). Physicochemical properties of glycine-based ionic liquid [QuatGly-OEt][$EtOSO_3$](2-ethoxy-1-ethyl-1,1-dimethyl-2-oxoethanaminium ethyl sulfate) and its binary mixtures with poly (ethylene glycol)(Mw= 200) at various temperatures. *International Journal of Molecular Sciences*, *12*(12), 8750–8772. doi:10.3390/ijms12128750

Wu, T. Y., Su, S. G., Wang, H. P., & Sun, I. W. (2011). Glycine-based ionic liquids as potential electrolyte for electrochemical studies of organometallic and organic redox couples. *Electrochemistry Communications*, *13*(3), 237–241. doi:10.1016/j.elecom.2010.12.022

Yahia, E. M. (2018). *Fruit and vegetable phytochemicals: Chemistry and human health* (Vol. II). John Wiley & Sons Ltd.

Yasuda, T., Bartlett, P. F., & Adams, D. J. (2008). Kir and Kv channels regulate electrical properties and proliferation of adult neural precursor cells. *Molecular and Cellular Neuroscience*, *37*(2), 284–297. doi:10.1016/j.mcn.2007.10.003

Yee, S. (1997). In vitro permeability across Caco-2 cells (colonic) can predict in vivo (small intestinal) absorption in man—Fact or myth. *Pharmaceutical Research*, *14*(6), 763–766.

You, G., Morris, M. E., & Wang, B. (2014). *Drug transporters: Molecular characterization and role in drug disposition*. John Wiley and Sons.